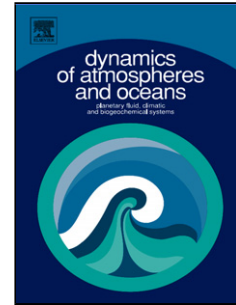# Accepted Manuscript

Title: The Makassar Strait Pycnocline Variability at 20-40 Days

Authors: Kandaga Pujiana, Arnold L. Gordon, E. Joseph Metzger, Amy L. Ffield

Please cite this article as: Pujiana, K., Gordon, A.L., Metzger, E.J., Ffield, A.L., The Makassar Strait Pycnocline Variability at 20-40 Days, {\it{Dynamics of Atmospheres and Oceans}} (2010), doi:10.1016/j.dynatmoce.2012.01.001

The Makassar Strait Pycnocline Variability at 20-40 Days

Kandaga Pujiana[1] and Arnold L. Gordon
Lamont-Doherty Earth Observatory, Palisades, New York

E. Joseph Metzger
Naval Research Laboratory, Stennis Space Center, Mississippi

Amy L. Ffield
Earth & Space Research, Upper Grandview, New York

[1] Corresponding author address: Kandaga Pujiana, Lamont-Doherty Earth Observatory, 61 Route 9W, Palisades, NY 10964.
E-mail: kandaga@ldeo.columbia.edu
Phone/Fax:(845) 365-8608/(845) 365-8175

1

1   Abstract

2   The characteristics and plausible genesis of the 20-40 day variability observed within the

3   Labani Channel, a constriction within the Makassar Strait, Indonesia, are described. The

4   20-40 day variability, trapped beneath the depth of the strongest stratification of the

5   pycnocline, is most evident in the across-strait flow, and in the across-strait gradient of

6   the along-strait flow as well as in the vertical displacements of isotherms. The 20-40 day

7   energy distribution of the across-strait flow is identifiable as a blue spectrum,

8   demonstrating downward phase propagation. The flow fields are approximated by a

9   vortex velocity structure, and the corresponding isotherm displacements imply potential

10   vorticity conservation. We propose that the 20-40 day features observed in the Labani

11   Channel are expressions of cyclonic and anti-cyclonic eddies that are advected southward

12   within the Makassar Strait throughflow. Analysis of simulated eddy kinetic energy from

13   an eddy-resolving model further indicates that the upstream instability of the background

14   flow within Makassar Strait is the energy source for the eddies which are dissipated

15   within the Labani Channel.

16

17   Keywords: Makassar Strait, Indonesian Throughflow, intraseasonal variability, eddies,

18   eddy-resolving model

19

20

21

22

23

2

24 1. Introduction

25   Makassar Strait is the primary Pacific water inflow gateway to the Indonesian

26 Throughflow [ITF] (Fig. 1a; Gordon and Fine, 1996). Observations made during 2004-

27 2006 indicated that the Makassar Strait throughflow contributed 12 x 10^6 m^3/s to the ITF

28 total of 15 x 10^6 m^3/s (Gordon et al., 2008; Gordon et al., 2010). The Makassar Strait

29 throughflow is not steady but rich in interannual and seasonal variability as well as

30 energetic fluctuations at tidal and intraseasonal [<90 day period] timescales (Gordon et

31 al., 2010).

32   An earlier investigation of intraseasonal flow in Makassar Strait, using a 1.5 year

33 (1996-1998) time series of along-channel speeds at 300 m and 450 m, showed two

34 significant intraseasonal variability [ISV] peaks: 35-60 and 70-100 days (Susanto et al.,

35 2000). Estimates based on numerical experiments suggested that the two peaks were

36 directly linked to remote forcing emanating in the Western Pacific and Indian Ocean, as

37 well as baroclinic eddies originating in the Sulawesi Sea (Qiu et al., 1999; Masumoto et

38 al., 2001). The *International Nusantara Stratification and Transport* [INSTANT]

39 program from 2004 to 2006 (Sprintall et al., 2004; Gordon and Kamenkovich, 2010)

40 provides a longer time series with improved vertical resolution of the Makassar Strait

41 throughflow. The Makassar along-strait flow observed by the INSTANT program reveal

42 that the 45-90 days variability characterizes the intraseasonal motions in the Makassar

43 Strait pycnocline, and the vertical structure of the motions resembles that of remotely

44 forced baroclinic waves (Pujiana et al., 2009).

45   In this study we investigate the 20-40 day signatures within the Makassar Strait

46 pycnocline and focus the analysis on the across-strait flow (a parameter that has been

47 overlooked in previous studies), relative vorticity derived from the along-strait flow at the

48 two INSTANT moorings located across Makassar Strait and the temperature fluctuations.

49 Although the across-strait mean flow in Makassar Strait is smaller than the along-strait

50 mean flow (the maximum across-strait mean flow at the Labani Channel ~ $O(0.25 \text{ cm/s})$),

51 its variance exhibits some interesting aspects. For example, the flow fields at periods of

52 20-40 days show that the variances in the across-strait component are comparable or

53 larger than that in the along-strait direction at depths ranging from 100 to 300 m in the

54 Makassar Strait pycnocline. We propose that the pronounced 20-40 day variability in the

55 Makassar Strait pycnocline derives its momentum from cyclonic and anti-cyclonic

56 eddies, which are advected southward with the mean Makassar Strait throughflow. A

57 better understanding on the 20-40 day features provides a fuller picture of Makassar

58 Strait intraseasonal flow.

59 The presentation of this paper is organized as follows. We will first describe the

60 data employed in section 2. Section 3 covers general descriptions of the 20-40 day

61 variability and their corresponding eddy characteristics from several parameters observed

62 in the Labani Channel. This is then followed by discussion on the eddy genesis in

63 Makassar Strait as simulated by an eddy-resolving model in section 4. The last section

64 concludes the paper with discussion and summary.

65

66 2. Data

67 The INSTANT program observed the ITF by means of moorings with ADCPs,

68 current meters, and temperature sensors, deployed at several Indonesian passages linking

69 the Pacific to the Indian Ocean (Sprintall et al., 2004). For this study we will be using the

4

70   INSTANT data within Makassar Strait. We also utilize several Conductivity,

71   Temperature, Depth [CTD] casts from the Arus Lintas Indonesia [ARLINDO] program

72   of 1993-1998 (Gordon and Susanto, 1999) and simulated velocity vectors from the

73   HYbrid Coordinate Ocean Model [HYCOM] (Metzger et al., 2010).

74

75   2.1.   ADCP and Current Meter

76   The INSTANT 2004-2006 program monitored the ITF transport in Makassar Strait

77   from two moorings: 2°51.9' S, 118° 27.3 E [MAK-West] and 2°51.5' S, 118° 37.7' E

78   [MAK-East], within the 45 km wide Labani Channel (Gordon et al., 2008; Fig. 1a). Each

79   mooring consisted of an upward-looking RD Instruments Long Ranger 75 kHz Acoustic

80   Doppler Current Profiler [ADCP] at a depth of 300 m and four current meters deployed at

81   200, 400, 750, and 1500 m. The Mak-West and Mak-East moorings recorded ~3-year

82   long datasets from 2004 to late 2006. The datasets, horizontal velocity vectors, are

83   linearly interpolated onto a 25-m depth grid for each two-hour time step to produce

84   gridded current vectors from 50 to 450 m of water column. The gridded horizontal

85   current vectors are subsequently projected to the along (y) and across-strait (x) axis of the

86   Labani Channel, which are oriented along -10° and 80° (relative to north and positive is

87   clockwise) respectively (Fig.1a), to yield gridded along (v) and across-strait (u) currents.

88

89   2.2.   CTD

90   The CTD datasets used for this study are a compilation of several CTD casts

91   collected within or near Labani Channel during ARLINDO 1993-1998 cruises (Fig.1a).

92   For each station, a Neil Brown Instrument System Mark III [NBIS MK III] CTD

5

93   measured conductivity, temperature and pressure within 12 hours period, yielding CTD

94   casts or temporal variability of measured parameters. CTD was lowered at a rate of 1 ms⁻

95   ¹, and a 16 s⁻¹ sampling rate was selected. A phase lagging filter is applied to the

96   conductivity data as correction for the time constant mismatch. The data are then coarsely

97   de-spiked and reduced to a 1-dbar pressure series by applying a 5-scan median filter

98   around the target pressures.

99   A density profile inferred from several CTD casts within the Labani Channel shows

100   that the pycnocline layer occupies a small fraction of water column from ~25-450 m,

101   with the strongest stratification at mid-pycnocline near 125 m separating the upper (25-

102   100 m) and lower (150-450 m) pycnocline (Fig. 1b).

103

104   2.3.   Temperature Sensors

105   Several temperature and pressure sensors attached to Mak-West and Mak-East

106   moorings measured the temporal variability of the temperature profile in Makassar Strait.

107   Mak-West mooring provided better temperature profile resolution with 17 sensors

108   attached at different levels from 100 m to 400 m; Mak-East mooring only had 5 sensors.

109   The sensors sampled temperature and pressure at 6-minute intervals over a period of

110   almost 3 years from January 2004 to November 2006. The temperature datasets are

111   linearly interpolated onto a 25-m depth grid for each two-hour time step to provide the

112   gridded temperature data from 150 to 350 m of water column. Since the vertical structure

113   of temperature variability is less resolved at Mak-East mooring, we will only analyze the

114   temperature profile datasets from Mak-West.

115   To investigate the vertical structure of thermal field, mooring sensor temperature

116   data available in the lower pycnocline layer are converted to vertical displacement (η).

117   Neglecting horizontal advection, diffusion, and heat sources, η is calculated using a heat

118   equation, which is simply a ratio between the gridded temperature amplitudes and the

119   vertical gradient of the averaged temperature, $\eta(z,t) = T(z,t)/\partial T/\partial z$, where z and t denote

120   depth and time respectively. The averaged temperature is a mean of the entire ~3-year

121   datasets. To remove the static stability effect from η, we normalize η with the ratio

122   between stratification frequency structure (determined from the CTD data shown in

123   Figure 1b) and its corresponding vertical average, $\eta_n(z,t) = \eta(z,t)[N/N_o]$, where subscript

124   n and o are for normalized and vertically averaged respectively.

125

126   2.4.   Simulated Data

127   Simulated velocity vectors and temperature variability from a numerical ocean

128   model are also used in this study. HYCOM has a horizontal resolution of 1/12.5° cos(lat)

129   x 1/12.5° and employs 32 hybrid vertical coordinate surfaces with potential density

130   referenced to 2000 m. It has been shown to realistically simulate the circulation pathways

131   of the Indonesian Seas, and specific model formulation details can be found in Metzger et

132   al. (2010). We examine daily data for a 3-year period from 2004 to 2006 within the

133   Makassar Strait pycnocline, where the data are gridded vertically with a uniform

134   resolution of 25 m from the surface to 450 m of water column.

135

136   3.   Description of the intraseasonal velocity and thermal fields

137   In this section, general characteristics of the Labani Channel velocity and

138 temperature profile variability measured are described. The statistical methods used to

139 explore those characteristics are mainly spectral method, cross-correlation in frequency

140 domain, and complex principal component analysis.

141

142   3.1.   Observation

143   3.1.1. Horizontal and Sheared Flows

144   Gordon et al. (2008) using INSTANT data from 2004 to 2006 reported the vertical

145 and horizontal profiles of the Makassar Strait mean flow for sub-tidal variability and

146 found that $\overline{v}$ revealed a distinct maximum southward (-y) speed at 140 m with western

147 intensification. The average direction of the flow points slightly to the east of

148 approximately north-south along-axis direction. Superimposed on the mean flow are the

149 fluctuations (u' and v') across a broad spectrum from inertial to interannual time frame.

150 Focusing on the intraseasonal variability and investigating the vertical profile of the

151 variance attributed to along-strait and across-strait flow, $\overline{u'^2}$ and $\overline{v'^2}$, where over bar

152 delineates integration over intraseasonal periods, we find that the profile exhibits: the

153 maximum $\overline{u'^2}$ is found at mid pycnocline (Fig. 2a), while $\overline{v'^2}$ attains maximum

154 magnitude at depth closer to the sea surface (Fig. 2b). The ratio between $\overline{u'^2}$ and $\overline{v'^2}$

155 suggests that the intraseasonal motions are anisotropic throughout the Mak-West

156 pycnocline depths (Fig. 2c), and $\overline{u'^2} > \overline{v'^2}$ for $75 \leq z \leq 225$ m. If the ratio were derived for

157 motions with periods of 20-40 days only, the depths where $\overline{u'^2} > \overline{v'^2}$ would then extend

158   from 75 to 275 m (not shown). Meanwhile Mak-East mooring shows that $\overline{u'^2} > \overline{v'^2}$ is

159   restricted to a thinner water column from 100 to 150 m (Fig. 2c).

160   The structure of variances for both velocity components versus depths (Fig. 2)

161   likely reflects the dynamics of the intraseasonal motions at the Labani Channel. For

162   example, a topographically trapped baroclinic Kelvin wave, a forcing that theoretically

163   requires small transverse flow, may explain stronger signatures of $v'(z)$ at depths beneath

164   225 m. An analysis of v' at intraseasonal periods over pycnocline depths in Makassar and

165   Lombok Straits suggests that remotely forced baroclinic waves propagate from Lombok

166   to Makassar Strait in the lower pycnocline depths (Pujiana et al., 2009). On the other

167   hand, robust signatures of u' at intraseasonal timescales over depths of 75-225 m maybe

168   driven by a topographic Rossby wave or an advected eddy whose dominant signal is

169   expected to be in the normal component or x-direction at the Labani Channel.

170   A spectral analysis is applied to the datasets to examine which periods within

171   intraseasonal timescales dominate the flow field variances in the Makassar Strait

172   pycnocline. The power spectrum is computed using the multi-taper method with adaptive

173   weighing. Two distinct spectral peaks, 20-40 days and 45-90 days, generally characterize

174   the intraseasonal flows in the Makassar Strait pycnocline. The 45-90 day variability is a

175   dominant feature in v' for throughout the pycnocline depths and extracts most of its

176   energy from remotely forced baroclinic waves (Pujiana et al., 2009).

177   As for the 20-40 day variability, v' shows strong signature at 100-150 m of the

178   Mak-West water column, where the flow is well defined by a spectral peak centered at

179   30-day (Fig. 3a). A distinct monthly spectral peak is absent beneath 150 m of the Mak-

180   West pycnocline although the 20-40 day variability energy does not change substantially

181   with depth. Some discrepancies are found from the Mak-East pycnocline, however, in

182   which the spectral peak centered at a shorter period of 25-day is more dominant and

183   occurs deeper in the lower pycnocline from 225 to 300 m (Fig. 3b). Furthermore, relative

184   vorticity (ζ') computed from v' of both moorings, shows significant variance associated

185   with monthly variation. A broad spectral peak of 20-40 day centered at a period of 30-day

186   characterizes ζ' at depths that extend from the base of the upper pycnocline to the lower

187   pycnocline layer, and its energy is comparable or larger than that attributed to the 45-90

188   day variability (Fig. 3c).

189   The signature of the 20-40 day variability over the Makassar Strait pycnocline is

190   more pronounced in the u' data. The vertical distribution of energy density of u' at Mak-

191   West across intraseasonal frequencies for several depths (Fig. 4a) indicates that the

192   spectrum shape transforms from red to blue spectrum as depth increases from 100 to 175

193   m; a blue spectrum with a distinct spectral peak centered at 25-day gains energy with

194   depth. Deeper in the lower pycnocline, the spectral peak of the 20-40 day variability

195   tends to be centered at a longer period of 30-day. The Mak-East mooring also shows a

196   similar pattern of the 20-40 day variability in the lower pycnocline (Fig. 4b). The 20-40

197   day variation observed from the Mak-East is also linked to that observed from the Mak-

198   West as more than 80% of variance attributed to the 20-40 day variability from both

199   mooring is statistically coherent. In addition to being coherent, the 20-40 day variability

200   from the two moorings does not exhibit a significantly different from zero phase shift, a

201   fact which may indicate that the 20-40 day variability has its horizontal scale across the

202   strait larger than the ~19 km distance separating the moorings.

203   Distinct 20-40 day spectral peaks marking u' and ζ' may express turbulent

204 fluctuations on the mean flow that transports momentum across the strait. The

205 instantaneous rate of along-strait momentum transfer in the across-strait direction is

206 defined as $\rho_o (V + v')\, u'$, where V is the mean flow, and u' and v' are velocity fluctuations

207 in the across-strait and along-strait directions respectively. The average rate of flow of

208 along-strait momentum in the across-strait direction is therefore

209 $\rho_o \overline{(V + v')u'} = \rho_o V\overline{u'} + \rho_o \overline{v'u'} = \rho_o \overline{v'u'}$, as $\overline{u'} = 0$. The Reynolds stress, $\rho_o\overline{v'u'}$, is

210 approximated with a cross-correlation between v' and u'. Structure of $\overline{v'u'}$, normalized by

211 their variances and averaged over intraseasonal periods shows that $\overline{v'u'} < 0$ (Fig. 5a),

212 which implies a westward (eastward) eddy flux of southward (northward) momentum.

213 And the correlation coefficient in frequency domain (Fig. 5b) indicates that the 20-40 day

214 variability contributes substantially, particularly that in the lower pycnocline.

215   Another way to interpret $\overline{v'u'} < 0$ is in terms of the turbulence. The vertical

216 structure of the mean flow (the time average of subinertial flow) observed at the

217 Makassar Strait moorings indicates that the flow is directed southward and found with a

218 maximum within the Mak-West pycnocline below 50 m (Fig. 5c). More energetic Mak-

219 West flow yields positive mean zonal shear and relative vorticity ($\partial\overline{v}/\partial x > 0$). Assume

220 that a particle at a point between Mak-West and Mak-East sites instantaneously moves

221 eastward ($u'>0$). The particle retains its original velocity during the migration, and when it

222 arrives at Mak-East it finds itself in a region where a smaller velocity prevails. Thus the

223 particle tends to speed up the neighboring fluid particles after it has reached the Mak-East

224 site, and causes a more negative (southward) v'. Conversely, the particles that travel

225 westward ($u' < 0$) tend to drag v' down. In this way turbulence tends to diffuse and

226 attenuate the across gradient of the mean flow, $\partial \overline{v}/\partial x > 0$.

227   Another unique feature from u' varying at periods of 20-40 days, which is

228 synonymously observed from both mooring, is a pattern of phase shift over depths:

229 $u'(z+dz)$ tends to flow slower than $u'(z)$ with a constant lag. On a time and depth plot of u'

230 at a 20-40 day period band (Fig. 6a), we draw lines, where each line connects the flow

231 that has the same phase, i.e. phase lines. And those lines are uniformly tilted downward at

232 an almost constant angle, indicative of a downward phase propagating feature. This

233 downward phase shift found from u' differs from the phase shift of dominant variability

234 in v'. Pujiana et al. (2009) suggested that the most dominant period band of v' observed in

235 the Makassar Strait pycnocline exhibited upward phase propagation, which transferred

236 energy downward to deeper depths at a speed of 25 m/day. A complex principal

237 component (CPC) analysis of u' varying at timescales of 20-40 days indicates that up to

238 90% of variances can be explained by the first three eigenvectors, where the first mode

239 describes 50% variance and the next two modes denote 25% and 15% variance

240 respectively. From the eigenvector profile, we learn how the amplitudes of u' vary with

241 depth. The first mode eigenvector reveals maxima at 175 m and at 250 m (Fig. 6b) where

242 two distinct spectral peaks of 25-day and 30-day are also observed: the energy associated

243 with the spectral peak centered at 25-day is maximum at depth of 175 m, while the

244 energy attributed to the 30-day variability is maximum at depth of 250 m. Therefore the

245 vertical energy distribution for the 20-40 day across-channel flow is well resolved by the

246 first eigenvector. Moreover, the relative phase inferred from the ratio between the

247 imaginary and the real part of the first eigenvector signifies a phase increase with a rate

12

248 of 1.7°/m towards greater depths (Fig. 6b). The rate of phase shift implies that it would

249 take around 20 days for the 25-day oscillation to propagate from 125 m to 300 m of water

250 column. This relative phase structure is better understood from reconstructed data

251 obtained through a multiplication between eigenvectors and their corresponding principal

252 components (time series). A plot of reconstructed u' based on eigenvector and principal

253 component for the first mode captures the phase shift nature revealed by the eigenvector

254 profile: periodic 20-40 day variability with phase lines titled downward at a uniform

255 angle (Fig. 6c). Thus the unique downward phase propagation feature contained in the

256 filtered 20-40 day u' data can be resolved and replicated by only the first mode.

257

258 3.1.2. Vertical displacement

259   The vertical displacement of the isotherms within Makassar Strait is rich in

260 intraseasonal features (Fig. 4c). Figure 4c demonstrates that significant variance

261 associated with 25-day oscillation also characterizes temperature fluctuations at 150 m

262 and greater depths. The vertical scale of the temperature variability within a period band

263 of 20-40 days is likely larger than the lower pycnocline thickness, as the correlation

264 between temperature variability at different depths shows that 70% temperature variance

265 at 150 m is coherent with that at 300 m (not shown). Thermal field at intraseasonal

266 timescales within Makassar Strait shares a similar power spectrum pattern with the

267 across-strait flow data as the variability shows significant 20-40 day variation, and it is

268 likely that the two parameters are physically linked.

269

270 3.1.3. Eddy-like features from observation

13

271   In previous sections we have discussed general characteristics of the 20-40 day

272   variability in the Makassar Strait pycnocline extracted from datasets obtained at the

273   Labani Channel of Makassar Strait. At least three interesting features attributed to the 20-

274   40 day variability were obtained from the datasets.

275   1. The u' is more energetic than v' at depths extending from 100 m to 250 m.

276   Although inferring the two-dimensional motion from two points is inherently tricky, we

277   suspect that a dominant across-strait flow at the Labani Channel may relate to an eddy

278   advected by the ITF. Assume an eddy propagates along a mean flow, $U(t) + iV(t)$, that is

279   spatially uniform but varying with time, the eddy's path can be projected into a complex

280   plane as $x'(t) + iy'(t) = r'(t)e^{i\varphi(t)}$. The currents observed by a mooring are then given as

281   (Lilly and Rhines, 2001)

282        $$\xi(t) = V + iU - ie^{i\varphi}v(r)$$ (1)

283   where $v(r)$ is the radial velocity of the eddy and r is the distance from the mooring to the

284   eddy center. If the eddy dynamics is simplified as a Rankine vortex, $v(r)$ can be

285   expressed in the following formula

286        $$v(r) = \begin{cases} VrR^{-1}, r < R \\ Vr^{-1}R, r > R \end{cases}$$ (2)

287   where V is the maximum azimuthal velocity, and R marks the eddy core radius that has

288   uniform potential vorticity. Since the ITF flows in the y-direction at the Labani Channel,

289   the observed eddy currents, by virtue of eq. (1) and (2), then are always perpendicular to

290   the along-strait axis or in the across-strait component. Therefore, the observed flow

291   associated with the eddy would be more dominant in u' than in v'.

292   2. There are 17 $+\zeta'$ and 18 $-\zeta'$ events over ~3 year observation at which the v' data

293   in Mak-West and Mak-East moorings are in opposite directions: $+\zeta'$ occurs when $-v'$ at

294   Mak-West and $+v'$ at Mak-East are observed, while $-\zeta'$ appears when $+v'$ at Mak-West

295   and $-v'$ at Mak-East are observed (Fig. 7, upper panel). Given the Mak-West and Mak-

296   East moorings are separated by a distance of ~19 km across a ~60 km width channel (Fig.

297   1b), the current vector in opposite senses that mark the positive and negative relative

298   vorticity phases may imply that the moorings are located on different side of the passing

299   eddies. To better visualize the relationship between the out of phase signature of v

300   observed at the two moorings and an eddy, it is shown in Figure 7 (lower panel) an ideal

301   vortex, whose azimuthal velocity structure is given in eq. (2), has a core with radius

302   presumably of 20 km and its center assumed on the median line of the Labani Channel. It

303   thus can be inferred from Figure 7 (lower panel) that the out of phase nature shown by

304   the v' timeseries at 20-40 days (Fig. 7, upper panel) may relate to eddies whose center

305   likely occurs in between the two moorings.

306   3. The strongest $+\zeta'$ episodes, at which $-v'$ at both moorings is out of phase, are

307   preceded with $+u'$, while $-\zeta'$ events coincide with initially observed $-u'$ (Fig. 8a,b). We

308   argue that the relationship between u' and ζ' measured in the Labani Channel consistent

309   with what a mooring would observe from a passing eddy as suggested by Lilly and

310   Rhines (2002): Normal component of eddy currents is initially positive (negative) for an

311   anticlockwise (clockwise) eddy. To further examine whether the nature of u' is linked to

312   eddy footprint at the moorings, we examine a Rankine vortex on Eulerian current records,

313   which the associated currents can be written as

314
$$\xi'(t) = \begin{cases} -iR^{-1}V\chi \\ -i\chi^{-1}VR \end{cases}$$
(3)

315 where χ is the distance from the mooring location to the eddy center. We assume that V

316 (the peak azimuthal speed at the eddy edge) is 15 cm/s, the southward advection speed of

317 the vortex is 20 cm/s, the eddy core radius is 20 km, and the eddy center is set at about 31

318 km to the north of the measurement points for the initial condition. Also the isobaths are

319 presumably perpendicular to the mooring transect, and the moorings are placed across a

320 50 km-wide channel in a way that replicates mooring arrangements in the Labani

321 Channel. We run the eddy model with the same eddy parameters for both anticlockwise

322 and clockwise eddies but change the sign of V from positive to negative for the clockwise

323 eddy case. The simulated eddy currents, either for anticlockwise or clockwise eddy, yield

324 a decent agreement with observations: the passing of a clockwise eddy ($-\zeta'$) is initially

325 marked with westward currents ($-u'$) (Fig. 8c), while the occurrence of an anti-clockwise

326 eddy ($+\zeta'$) is preceded by the onset of eastward currents ($+u'$) (Fig. 8d). A good

327 accordance between real and theoretical events further indicates that the rotational events

328 observed from moorings in the Labani Channel are likely related to eddy motions.

329   4. The thermal field and relative vorticity are linked at the Labani Channel. The

330 isopycnals in the lower pycnocline layer dip down when the flow field exhibits negative

331 relative vorticity (Fig. 9a). Meanwhile the isopycnals shoal as the relative vorticity

332 observed in the Labani Channel lower pycnocline turns positive (Fig. 9b). We suspect

333 that the vertical displacements of isopycnals varying at periods of 20-40 day in the lower

334 pycnocline of the Labani Channel are direct responses to water column squeezing or

335 stretching attributed to cyclonic or anti-cyclonic eddies, attributable to potential vorticity

336 conservation. Potential vorticity conservation suggests that $(\zeta_{t0} + f)/h_{t0} = (\zeta_t + f)/h_t$,

337   where h is the isopycnal depth, and subscripts t_0 and t denote initial condition (at rest) and

338   time when an eddy passes the mooring sites. Assuming $\zeta_{t_0} = 0$, h_t at the mooring sites

339   located in the southern hemisphere can be written as $h_t = h_{t_0} (1 - (\zeta_t / f))$, it can be inferred

340   that the isopycnals are displaced upward (downward) when a motion with positive

341   (negative) relative vorticity passes through the mooring sites or the pycnocline shoals

342   (deepens) when an anticyclonic (cyclonic) eddy is advected through the observational

343   sites.

344   After reviewing the observations discussed in previous sections, we hypothesize

345   that the features attributed to the 20-40 day variability from the moorings at the Labani

346   Channel are linked to eddy dynamics, and the next step is to describe where the eddies

347   originate from. Several numerical experiments (Qiu et al., 1999; Masumoto et al., 2001)

348   indicated that eddy activities at intraseasonal timescales are intense within the Sulawesi

349   Sea, a basin located to the north of Makassar Strait (Fig. 1a). Masumoto et al. (2001)

350   estimated that eddies with a period of 40-day were internally generated in Sulawesi Sea

351   and affected the ITF transport in Makassar Strait. However the Sulawesi eddies that the

352   study of Masumoto et al. (2001) numerically estimated were not only trapped in the

353   lower pycnocline but rather occupied a thick water column extending from the surface to

354   1000 m isobath. To investigate the generating mechanism of eddies at the Labani

355   Channel, we analyze the output of an eddy resolving numerical models in Makassar

356   Strait, and the discussion is given in the following section.

357

358   4.   The 20-40 day variability in an eddy-resolving model

359   As described earlier, flow and thermal field from two moorings at the Labani

360   Channel of Makassar Strait reveal clear 20-40 day variability features, which we propose

361   are related to cyclonic and anti-cyclonic eddies. To further examine the spatial variation

362   and origin of the 20-40 day variability, we investigate the model output of a global

363   HYCOM experiment (Metzger et al., 2010). We focus our analysis on the model flow at

364   intraseasonal timescales in the Makassar Strait and Sulawesi Sea pycnocline. Comparison

365   between the model output and observation at the Mak-West and Mak-East mooring sites

366   indicates that the numerical experiment underestimates the Makassar Strait throughflow

367   due to inaccurate model topography, where the Dewakang Sill (Fig. 1a), located near the

368   southern end of the strait, was introduced 195 m too shallow in the model (Metzger et al.,

369   2010). In addition to weaker simulated mean transport, the study of Metzger et al. (2010)

370   also showed that shallower sill depth assigned in the model caused the maximum

371   simulated southward flow in Makassar Strait to be ~50 m deeper than observed.

372   The model u' at intraseasonal timescales qualitatively agrees with observation at

373   Mak-West and Mak-East moorings: the 20-40 day variability has clearly larger energy

374   than other intraseasonal periods, and the variability at Mak-West is more energetic than

375   that at Mak-East (Fig. 10a,b). It is also shown in Figure 10a,b that the distinct monthly

376   spectral peak is well simulated at depths greater than 200 m, which is 50-75 m deeper

377   than the depth where observation starts to record the monthly peak. The discrepancy is

378   again due to inaccurate sill depth. Monthly variation also occurs in the model ζ' simulated

379   at the mooring locations. Like the observation, the model ζ' and u' at depths beneath 200

380   m are linked: positive relative vorticity correlates with eastward flow, while negative

381   vorticity corresponds with westward flow (not shown). A coherence analysis between the

382   model ζ' and u' for several depths within the pycnocline layer of Mak-West site displays

383   that both parameters varying at intraseasonal timescales are strongly coherent for a period

384   band of 20-40 days, and the strongest correlation is found at depths greater than 200 m

385   (not shown). Moreover the simulation not only qualitatively shows a good agreement

386   with observation but also quantitatively explain significant variances of the recorded

387   datasets. It is inferred from some cross-correlation analyses between the simulated and

388   observed data at some select levels within the lower pycnocline depths that the model u'

389   explains 64-72% variances of the observed u' varying at 20-40 days. Thus the numerical

390   experiment is able to capture some general features of the 20-40 day variability, which

391   are similarly revealed from observation at the mooring sites in the Labani Channel.

392

393   4.1.   Eddy signature and its genesis in Makassar Strait

394   The next questions we explore within the model output are what causes the 20-40

395   day variability? Where does the forcing originate from? And why is the strong 20-40 day

396   variability trapped within the lower pycnocline. To determine the ocean dynamics

397   responsible for the pronounced 20-40 day fluctuations, the simulated flow field attributed

398   to the period band of interest in the Makassar Strait is analyzed. We first want to gain

399   insights on the space and time evolution of a motion that may drive the ζ' fluctuations in

400   Makassar Strait. For example, an event of positive ζ' is inferred from two moorings at

401   250 m in the Labani Channel on 17 December 2005 (selected to be representative of

402   positive ζ' events), and it is assumed that an anticlockwise eddy-like motion causes the ζ'

403   field. The model agrees well with observation to simulate positive ζ' at 250 m of the

404   Labani Channel pycnocline on 17 December 2005, and the model flow field shows that

19

405 the positive ζ' value does correspond with a counter clockwise vortex motion with a

406 diameter of ~40 km squeezed in the narrow Labani passage (Fig. 11). Assume quasi-

407 geostrophic dynamics govern the vortex observed and simulated in the Labani Channel,

408 the vortex diameter will be approximately as large as the local internal radius

409 deformation, which is function of N, coriolis acceleration (f), and water depth (H). The

410 deformation radius for the first oceanic mode in the Labani Channel falls within O(~275

411 km), substantially larger than the channel width itself. Therefore the eddy size in

412 Makassar Strait is more likely topographically constrained. The model velocity and

413 relative vorticity fields at the Labani Channel for over a period of ~3 years (2004-2006)

414 display 23 events of anti-cyclonic vortex motion and 17 episodes of cyclonic eddy-like

415 features.

416   Furthermore, following the spatial and temporal eddy core variability, it can be

417 inferred that the eddy-like motion is not locally generated at the Labani Channel but

418 seems rather to propagate from the northern Makassar Strait into the Labani Channel. It is

419 shown in Figure 11 that an anti-cyclonic eddy with a diameter of ~100 km has its core

420 located at latitude of 2°S and is simulated on 7 December 2005, and the eddy diameter is

421 reduced as it propagates southward with a phase speed of 0.25 m/s before occupying the

422 Labani Channel on 17 December 2005. After reaching the Labani Channel, the eddy

423 dissipates and its signature is not simulated further south (not shown).

424   The model eddy occurs only within the lower pycnocline and is identifiable as a

425 feature that has homogeneous ζ' over depths. A depth versus distance plot of ζ' along a

426 transect given in Figure 1 shows that a homogeneous positive ζ' over depths extending

427 from 200 to 350 m marks the event of an anti-cyclonic eddy on 17 December 2005 in the

428   Labani Channel (Fig. 12). Thus the eddy varying at periods of 20-40 days in Makassar

429   Strait is trapped within the lower pycnocline. Several snapshots of simulated horizontal

430   flow fields and structure of ζ' in Makassar Strait (Fig.11, 12) provide spatial and temporal

431   dimension of the motions that likely force the 20-40 day variability observed at the

432   Labani Channel. It is shown that circular motions develop at 2ºS or farther north and

433   propagate southward in Makassar Strait. To better map out the source region of the

434   vortices, we analyze simulated eddy kinetic energy (EKE) budget over an expanded

435   region including the Sulawesi Sea (Fig. 1), a basin with robust intraseasonal activities

436   (Qiu et al., 1999; Masumoto et al., 2001, Pujiana et al., 2009). Although detecting energy

437   radiation through EKE can be ambiguous, the intraseasonal variability can be

438   characterized by a suitably specified EKE.

439   The EKE budget is deduced from the rapidly-varying segment of u and v, with an

440   assumption that each variable has a slowly-varying part and a rapidly-varying part,

441   labeled as (u, v) and (u', v') respectively. The rapidly-varying part oscillates at periods of

442   20-40 days, and the EKE density is therefore defined as $0.5\rho_o(u'^2+v'^2)$, where ρ_o is the

443   background density, vertically averaged over depths from the potential density structure

444   given in Figure 2. Comparison of the averaged EKE (Fig. 13) at several depths clearly

445   exemplifies the basins with the most pronounced EKE in the region: Sulawesi Sea (A),

446   northern Makassar Strait (B), and Southern Makassar Strait (C), where the Labani

447   Channel demarcates the separation between the northern and southern of Makassar Strait.

448   Nevertheless we consider basins A and B as the only viable energy source areas for eddy

449   activities at the Labani Channel as we expect the eddy to be advected, along with the ITF,

450   southward into the channel. In area A, the eddy activity is significant close to the surface

451 and decays away from it, and the eddy likely does not extract its energy from the wind

452 because the atmospheric perturbations over the area lacks a 20-40 days variability (not

453 shown). The eddy might instead relate to instabilities of the Mindanao currents occurring

454 on the eastern Mindanao coasts or be a Sulawesi basin scale response to the periodic

455 Mindanao currents (Qiu et al., 1999; Masumoto et al., 2001). In contrast, the EKE

456 vertical distribution in B shows a structure that is quite typical of the mean flow profile in

457 the Labani Channel (Fig. 5c), in which the maximum value is attained at the mid

458 pycnocline depth, where the vertical shear of the mean flow is strongest. The EKE in B is

459 strongest at 200 m and fades away with distance from that depth (Fig. 14a).

460   Considering how the EKE is distributed in Makassar Strait and Sulawesi Sea, we

461 propose that zone B, rather than area A in Sulawesi Sea, is the EKE source for generating

462 eddies that are trapped in the lower pycnocline and propagate into the Labani Channel. If

463 area B were the eddies source, southward dispersion of EKE should be well simulated by

464 the model. To detect if there is southward energy transfer from zone B, we evaluate the

465 time evolution of EKE at a depth of 225 m, a depth that has the largest averaged EKE

466 value (Fig. 14a). The EKE temporal variability along a band of latitudes within zone B

467 demonstrates a southward propagating with a phase speed of 0.2 m/s which closely

468 matches the propagation speed of an eddy (Fig. 14b). To a first approximation, it

469 therefore can be proposed that the eddy observed in the Labani Channel is not generated

470 in the Sulawesi Sea, but rather originating from just to the north of the channel in the

471 Makassar Strait at latitudes varying from 0.5ºS to 2ºS.

472   The next questions are why the eddy-like motions are formed at latitudes which fall

473 within range of 0.5°-2°S in the Makassar Strait lower pycnocline, and how are they

474 initiated? As mentioned in the earlier discussion on eddies characteristics from

475 observation, we argue that the eddy occurring at depths beneath the mid pycnocline layer

476 of Makassar Strait extracts its energy from the sheared mean flow. To support the

477 argument that the eddy generation may relate to the background flow, spatial variation of

478 the time averaged speeds in Makassar Strait at several depths within the pycnocline, is

479 studied. The background flow magnitudes at several different depths (Fig. 15)

480 synonymously display significant variations across Makassar Strait: the southward mean

481 flow is simulated speediest at and south of the Labani Channel and at depths of 150-200

482 m. Figure 15 also demonstrates a clear across-strait gradient of the mean flow particularly

483 at latitudes of 0.5°-2°S as weaker northward mean flow on the eastern end of the

484 Makassar Strait features against the energetic western-intensified southward mean flow.

485 And the across-strait gradient of the mean flow within that particular latitude band

486 reveals its maximum at 200 m, a depth where the EKE is noticeably largest as shown in

487 Figure 13. Given the sheared mean flow and the EKE equally exhibit strongest signature

488 at depth of 200 m, we propose that the background flow supplies the eddy energy through

489 a flow instability mechanism. Assuming the mean flow structure across the strait can be

490 described as an inviscid parallel flow, the two necessary criteria for instability of the flow

491 are: the basic background flow profile has at least a point of inflection (Rayleigh's

492 inflection point criterion), and the magnitude of vorticity of the background flow must

493 have a maximum within the region of flow, not at the boundary (Fjortoft's theorm). The

494 imaginary part of the Rayleigh's equation (Kundu and Cohen, 2004) , $c_i \int (\partial^2 V/\partial x^2 |\phi|^2 /|V-$

495 $c|^2)$ d$x = 0$, suggests that for the unstable case to hold ($c_i \neq 0$), $\partial^2 V/\partial x2$ (the mean flow

496 curvature) needs to change sign across the strait (x-direction). Focusing on the across-

497   strait profile of the mean flow at 200 m within latitudes of 0.5°-2°S in Makassar Strait

498   (Fig. 16), the profile shows one inflection point at each latitude that marks the mean flow

499   structure across the strait, which complies with the necessary criterion for instability

500   required by the Rayleigh's equation. Another criterion for instability derived from

501   Fjortoft's theorem (Kundu and Cohen, 2004), $\int (\partial^2 V/\partial x^2 (V - V_I)|\phi|^2/|V-c|^2) \, dx < 0$,

502   indicates that the mean flow must not only have at least one inflection point across the

503   strait but also have maximum vorticity away from the boundary. And Figure 16 also

504   demonstrates that the positive relative vorticity magnitude of the mean flow has a

505   maximum within the region of flow, which provides another indication that the

506   background flow instability simulated within latitudes of 0.5°-2°S in Makassar Strait

507   potentially generate the eddies.

508

509   5.   Discussion and Summary

510   We have described the characteristics of the 20-40 day variability observed at the

511   two INSTANT moorings deployed in the Labani Channel of Makassar Strait 2004-2006.

512   The variability is well identified from the u' datasets recorded below the central

513   pycnocline depth of 125 m, as a distinct spectral peak, which resembles a blue spectrum

514   shape over the intraseasonal timescales. Comparison between u' and v' demonstrates that

515   the across-strait component of the 20-40 day variability intraseasonal feature is more

516   energetic within the pycnocline. Additionally, the 20-40 day fluctuations of u' reveal

517   downward phase propagation with a speed of 25 m/day and vertical distribution of

518   energy, in which the flow at the mid pycnocline depth oscillates at shorter period than it

519   does at greater depths.

520   Apart from u', the 20-40 day variability is also evident from the temperature

521   datasets as η' continuously show monthly periodicity. The magnitude of η' is larger than

522   the lower pycnocline thickness, and η' move up and down in concert although a small

523   phase difference is observed over the lower pycnocline layer. Although the 20-40 day

524   variability is not prominent in v', it does typify the $\partial v'/\partial x$ variation over the lower

525   pycnocline depths. The $\partial v'/\partial x$ time series exhibit strong correlations with u' which leads

526   us to propose that the 20-40 day variability is linked to eddy-like features. As discussed

527   previously, the velocity structure of a theoretical vortex approximates well the

528   observations and the relationship between the measured parameters. Moreover the link

529   between ζ' and η', the isopycnals dip down (elevated) as the relative vorticity magnitudes

530   turn negative (positive) may also signify the presence and role of an eddy to conserve the

531   potential vorticity within the water column in the Labani Channel.

532   If an eddy forces the 20-40 day variability within the lower pycnocline layer, why

533   does the variability at the top of the lower pycnocline has strongest energy at a period of

534   25-day while the variability at the base of the lower pycnocline attains maximum energy

535   at a period of 30-day? In other word, the spectral peak attributed to the 20-40 day

536   variability is centered at periods varying from 25-day at the mid pycnocline depth to 30-

537   day at the base of the lower pycnocline depth. Here, we suggest a Doppler effect may

538   better explain the pattern in question than the motion's natural frequencies. Referring to

539   the general dispersion relation for gravity waves, natural frequencies of motions that a

540   strait inherently can sustain is inversely proportional to the strait's width, $\omega = ((\pi g(n+1)L^{-1})\tanh((n+1)\pi HL^{-1}))^{1/2}$

541    $^1)\tanh((n+1)\,\pi HL^{-1}))^{1/2}$ where H, L, g, and n denote water depth, strait's width, gravity

542   and mode number, respectively. The relationship between the natural frequency and the

543   strait's width thereby indicate that as strait's width decreases with depth, natural

544   frequencies (periods) would get larger (smaller) with depth as natural frequency is

545   inversely proportional to strait's width. However, this increasing natural frequency with

546   narrower width relationship does not fit well in the Labani Channel because the

547   dominating frequency gets smaller as the channel's width decreases with depth. Another

548   physical process that may explain increasing periods of fluctuations with depth is

549   Doppler phase shift. If the 20-40 day event is advected southward with the background

550   flow, the feature is advected into the mooring sites with varying speeds over depths,

551   following the vertical structure of the mean flow (Fig. 5c), which is maximum at the mid

552   pycnocline depth and decays with distance from this depth. As consequence, the observed

553   dominant period of oscillation at the mid pycnocline depth is shorter than that at deeper

554   levels in which the 20-40 day variability propagates at a slower pace.

555   An eddy-resolving model further supports that the 20-40 day variability observed in

556   the Labani Channel of Makassar Strait is driven by eddies. The model horizontal flow

557   and ζ' fields show that a positive (negative) ζ' event observed in the channel does

558   correspond with an anti-cyclonic (cyclonic) eddy that originates in Makassar Strait at

559   latitudes between $0.5°$-$2°S$, just to the north of the mooring site, a region with the largest

560   EKE. The EKE vertical distribution within this band of latitudes demonstrates strongest

561   EKE magnitude at depths greater than 200 m. The area and depths with the largest EKE

562   also coincides with the latitudes and levels at which the across-strait gradient of the

563   model background flow may provide the necessary energy for the eddy formation in

564   Makassar Strait.

565   To summarize, we suggest that a cyclonic or an anti-cyclonic eddy generated at

566 latitudes between 0.5°-2°S in Makassar Strait explains strong signatures of the 20-40 day

567 variability in the across-strait flow and the temperature fluctuations observed within the

568 lower pycnocline of the Labani Channel. The generation mechanism of the eddy is likely

569 through instability in which the required energy is supplied by the across-strait shear of

570 along-strait flow, marking the ITF. The eddy is trapped in the lower pycnocline because

571 those are depths the EKE and the sheared background flow is found most energetic. The

572 eddy propagates southward along with the ITF and dissipates its energy in the Labani

573 Channel.

574

575

576

577

578

579

580

581

582

583

584

585

586

587

27

601   References

602   Gordon, A.L. and Kamenkovich, V.M., 2010. Modelling and observing the Indonesian

603   Throughflow. A special issue of Dynamics of Atmosphere and Ocean. Dyn. Atmos.

604   Oceans, doi: 10.1016/j.dynatmoce.2010.04.003.

605   Gordon, A.L., Sprintall, J., Van Aken, H.M., Susanto D., Wijffels, S., Molcard, R.,

606   Ffield, A., Pranowo, W. and Wirasantosa, S., 2010. The Indonesian Throughflow

607   during 2004-2006 as Observed by the INSTANT program. Dyn. Atmos. Oceans,

608   doi: 10.1016/j.dynatmoce.2009.12.002.

609   Gordon, A.L. and Susanto, R.D., 1999. Makassar Strait Transport: Initial Estimate Based

610   on Arlindo Results. Mar. Tech. Society, 32, 34-45.

611   Gordon, A.L. and Fine, R. A., 1996. Pathways of Water between the Pacific and Indian

612   Oceans in the Indonesian Seas. Nature, 379, 146-149, doi: 10.1038/379146a0.

613   Gordon, A.L., Susanto, R.D., Ffield, A., Huber, B.A., Pranowo, W. and Wirasantosa, S.,

614   2008. Makassar Strait Throughflow, 2004 to 2006. Geophys. Res. Lett., 35,

615   L24605, doi: 10.1029/2008GL036372.

616   Kundu, P. K. and I.M. Cohen, 2004. Fluid Mechaniscs, New York: Elsevier.

28

617   Lilly, J.M. and Rhines, P.B., 2002. Coherent Eddies in the Labrador Sea Observed from a

618   Mooring. J. Phys. Oceanogr., 32, 585-598, doi: 10.1175/1520

619   0485(2002)032<0585:CEITLS>2.0.CO;2.

620   Masumoto, Y., Kagimoto, T., Yoshida, M., Fukuda, M., Hirose, N. and Yamagata, T.,

621   2001. Intraseasonal eddies in the Sulawesi Sea simulated in an ocean general

622   circulation model. Geophys. Res. Lett., 28(8), 1631-1634.

623   Metzger, E.J., Hurlburt, H.E., Xu, X., Shriver, J.F., Gordon, A.L., Sprintall, J., Susanto,

624   R.D. and Van Aken, H.M., 2010. Simulated and Observed Circulation in the

625   Indonesian Seas: 1/12° Global HYCOM and the INSTANT Observations. Dyn.

626   Atmos. Oceans, 57, 275-300, doi: 10.1016/j.dynatmoce.2010.04.002.

627   Pujiana, K., Gordon, A.L, Sprintall, J. and Susanto, R.D., 2009. Intraseasonal variability

628   in the Makassar Strait Thermocline. J. Mar. Res., 67, 757-777.

629   Qiu, B., Mao, M. and Kashino, Y., 1999. Intraseasonal Variability in the Indo-Pacific

630   Throughflow and the Regions Surrounding the Indonesian Seas. J. Phys. Oceanogr.,

631   29, 1599-1618, doi: 10.1175/1520-0485(1999)029<1599:IVITIP>2.0.CO;2.

632   Susanto, R.D., Gordon, A.L., Sprintall, J. and Herunadi, B., 2000. Intraseasonal

633   Variability and Tides in Makassar Strait. Geophys. Res. Lett., 27(10), 1499-1502,

634   doi: 10.1029/2000GL011414.

635   Sprintall, J., Wijffels, S., Gordon, A.L., Ffield, A., Molcard, R., Susanto, R.D., Soesilo,

636   I., Sopaheluwakan, J., Surachman, Y. and Van Aken, H., 2004. INSTANT: A New

637   International Array to Measure the Indonesian Throughflow. Eos Trans.

638   AGU, 85(39), doi: 10.1029/2004EO390002.

639

640   Figures
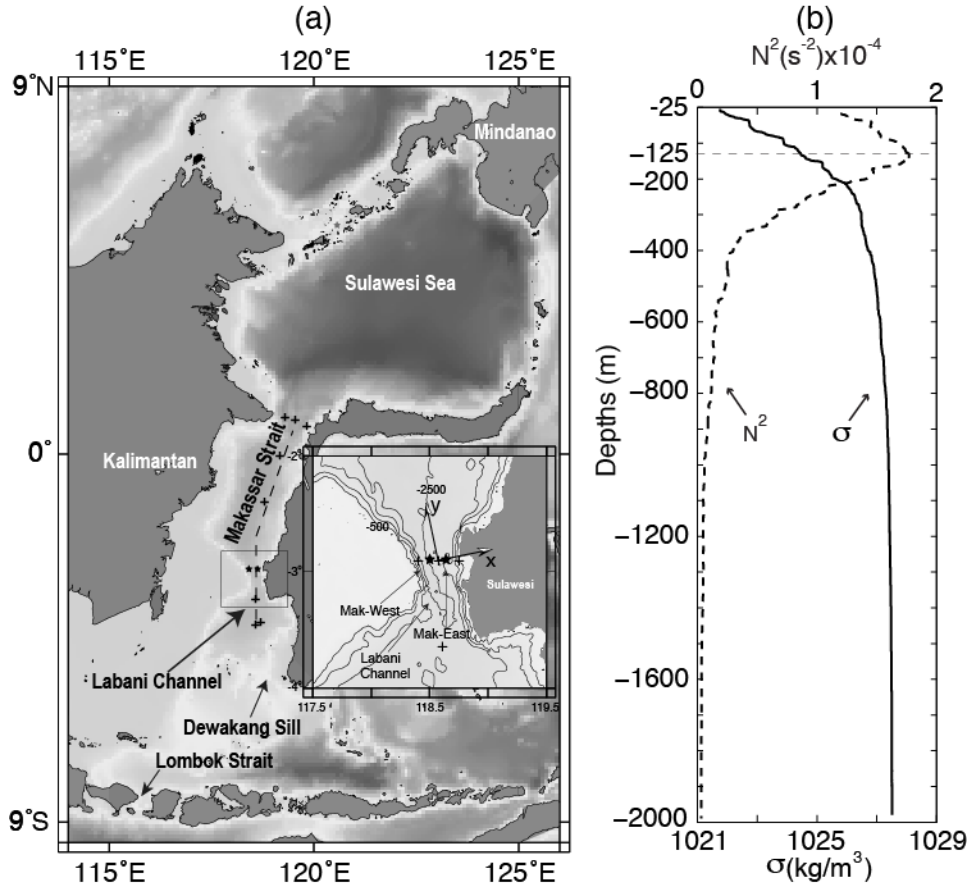
641

642   Figure 1. (a) Locations of point measurements in Makassar Strait. The moorings are

643   shown as stars and are deployed in the Labani Channel, a constriction in Makassar Strait.

644   Crosses denote CTD casts during 1996-1998. Inset displays an expanded view of the

645   Labani Channel, the major and minor axes of the channel, and the mooring sites (Mak-

646   West and Mak-East). The along-strait axis (y) and across-strait axis (x) is tilted 10°

647   counterclockwise relative to the geographic north and east respectively. (b) The average

648   vertical structure of the interior Makassar Strait inferred from several CTD casts during

649   1993-1998 given in Figure 1. The average of potential density (σ, solid line) and

650   buoyancy frequency (N^2, dashed line).

651
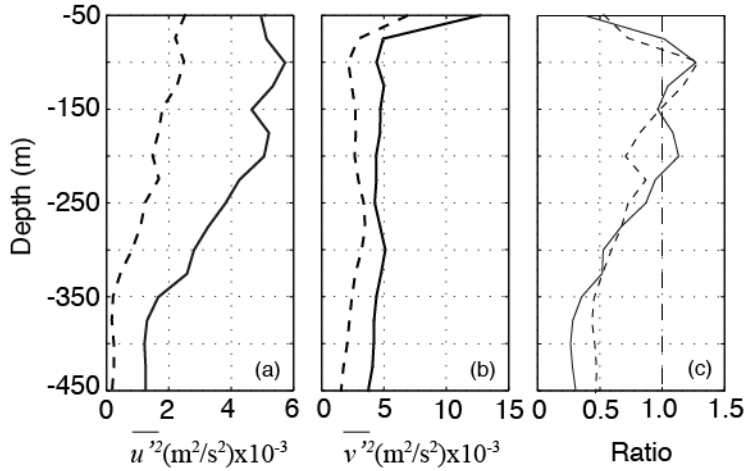
Figure 2. Profiles of variances attributed to u' (a) and v' (b) at intraseasonal timescales

(20-90 days) within the Mak-West (solid line) and Mak-East (dashed line) thermocline.

The corresponding ratio between u and v for each mooring (solid line: Mak-West; dashed

line: Mak-East) is given in (c).
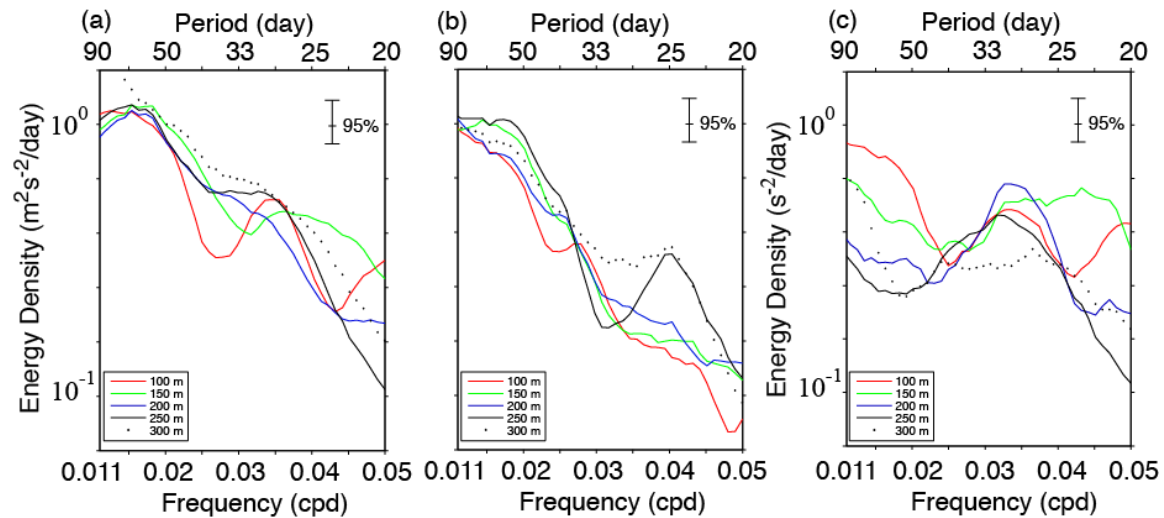
Figure 3. Multitaper spectral estimates of *v*' observed at different levels in the Mak-West

(a) and Mak-East (b) lower thermocline during 2004-2006. (c) displays spectral estimates

of across-strait gradient of *v*', computed by subtracting *v*' observed at Mak-East from that

observed at Mak-West. Error bars on the spectral estimates mark the 95% confidence

limits.

687
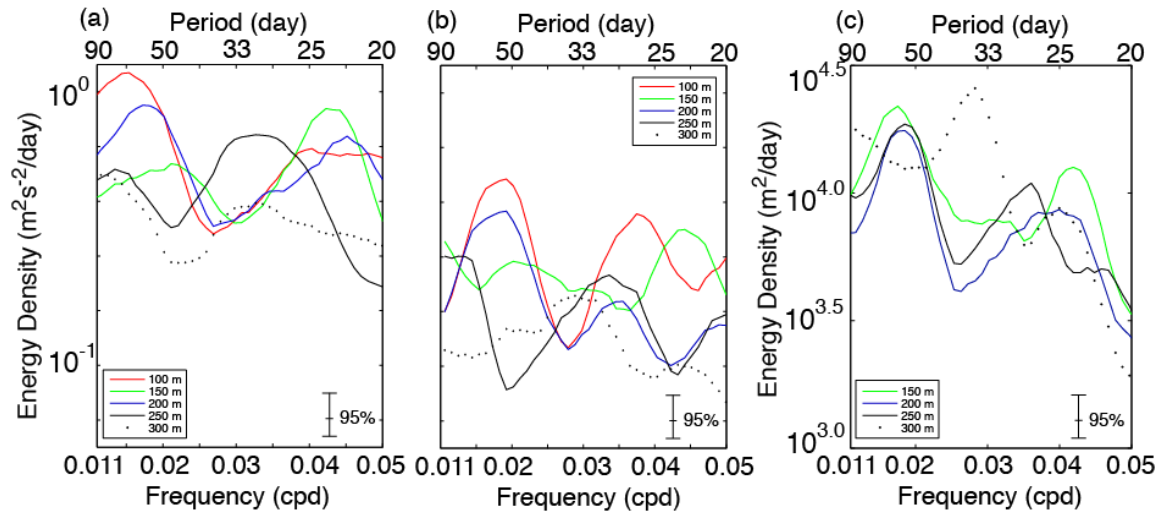
Figure 4. Multitaper spectral estimate of u' and η' at several levels from Mak-West and

Mak-East moorings within the lower thermocline of Makassar Strait during 2004-2006.

(a) and (b) illustrate spectral estimate of u' for Mak-West and Mak-East respectively. (c)

displays η' spectral estimates of for Mak-West. Error bars on the spectral estimates mark

the 95% confidence limits.

693

694

695

696

697

698

33
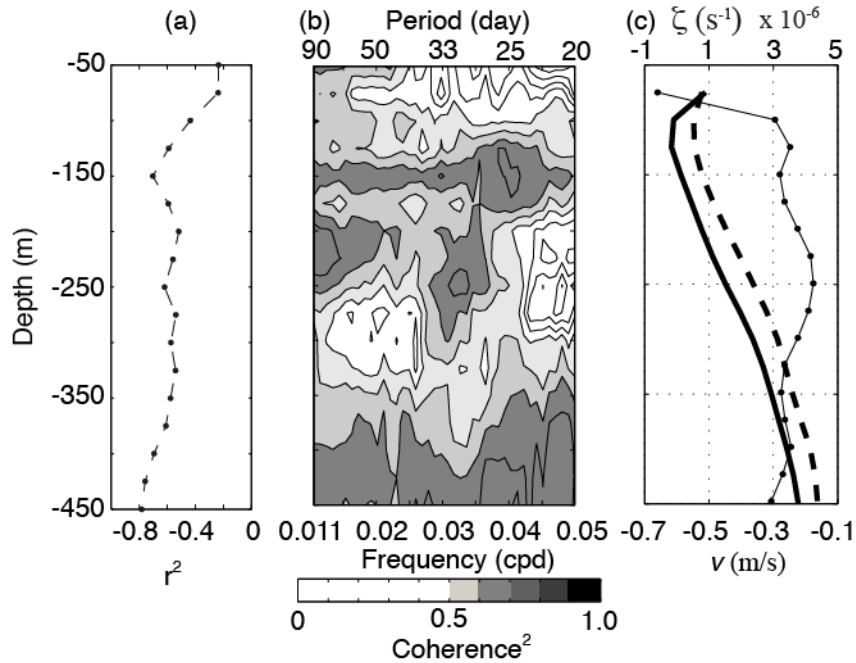
Figure 5. (a,b) The degree of correlation between v' and u' at intraseasonal timescales

over the Mak-West thermocline. (a) Zero-lag coefficients are obtained from time-lagged

cross correlation analysis. (b) Amplitudes of coherence squared are shaded for values

larger than 95% significance level. (c) Vertical structure of the background flow observed

at Mak-West (solid line) and Mak-East (dashed line) and its corresponding relative

vorticity (dotted line). The background flow at a certain depth is the time average of

subinertial flow, which is obtained through applying a butterworth low-pass filter to the

velocity field dataset with a cut-off period of 9.5-day (inertial period at the mooring site).

714
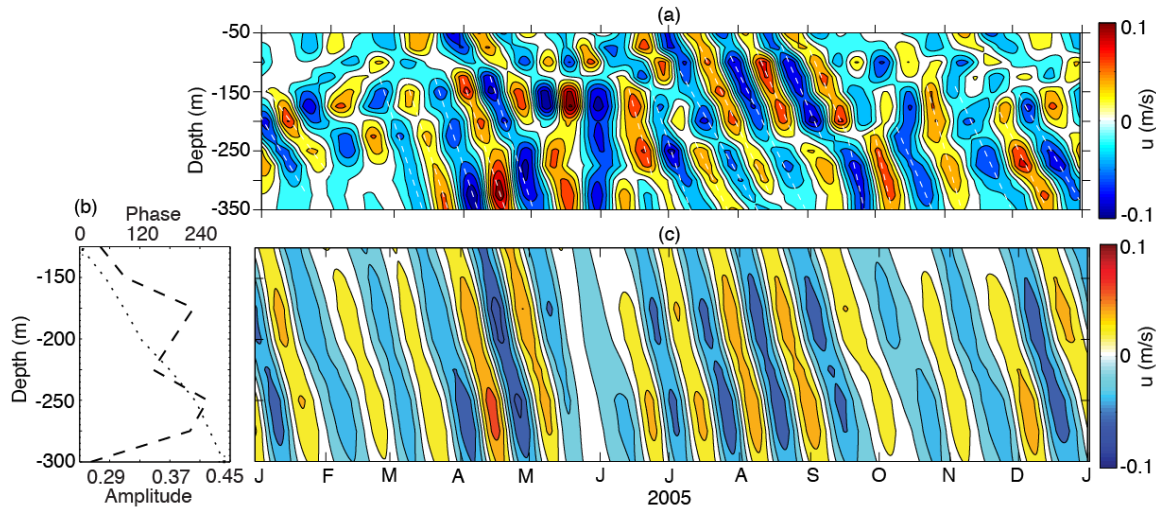
Figure 6. Across-strait flow varying at periods of 20-40 days observed at Mak-West

mooring in 2005 (a) and its orthogonal function approximation (b, c). Dashed lines in (a)

show phase lines. Dashed and dotted lines in (b) show the 1st eigenvector and its relative

phase that represents 50% variance of (a). (c): Reconstructed across-strait flow for the 1st

mode.

720

721

722

723

724

725

726

727

728

729

730

731
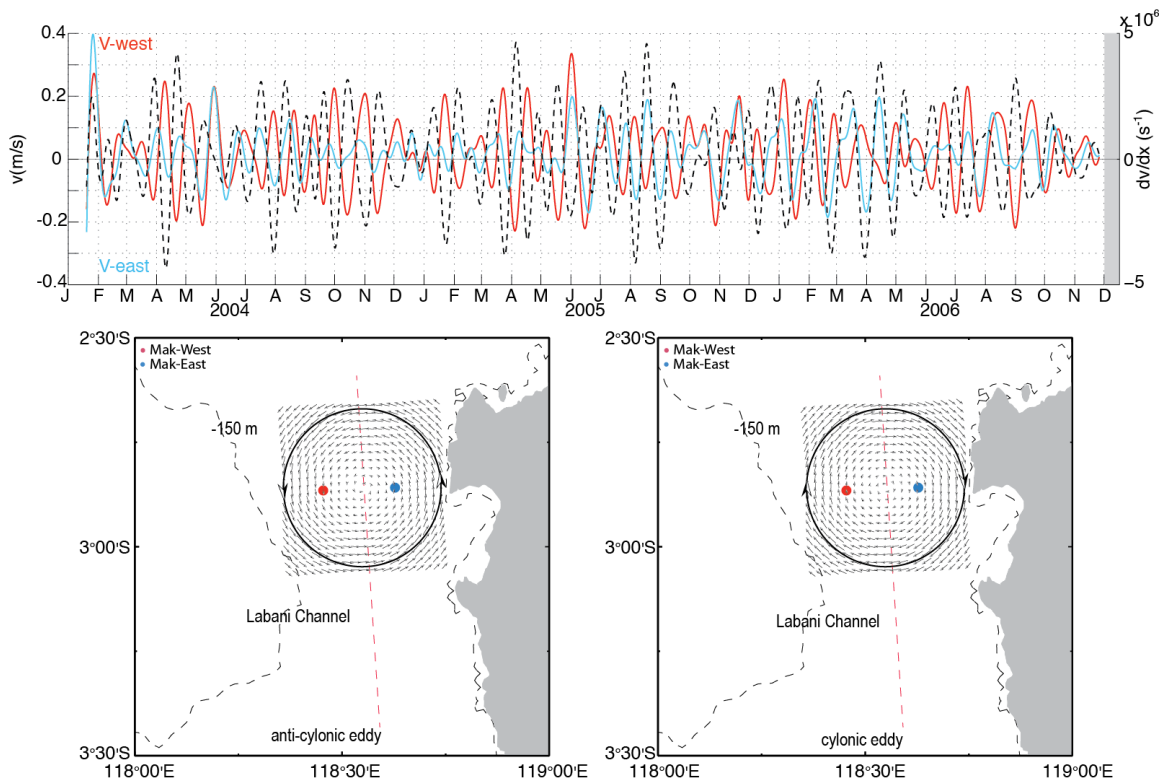
Figure 7. (Upper panel): Along-strait flow varying at 20-40 days and observed at depth of

150 m of the Mak-west (red) and Mak-East (blue) thermocline and the corresponding

dv/dx. (Lower panel): Illustration of ideal anticyclonic and cyclonic eddy currents in the

Labani Channel. Dashed red line denotes the median line of the Labani Channel.

736

737

738

739

740

741

742

743

744
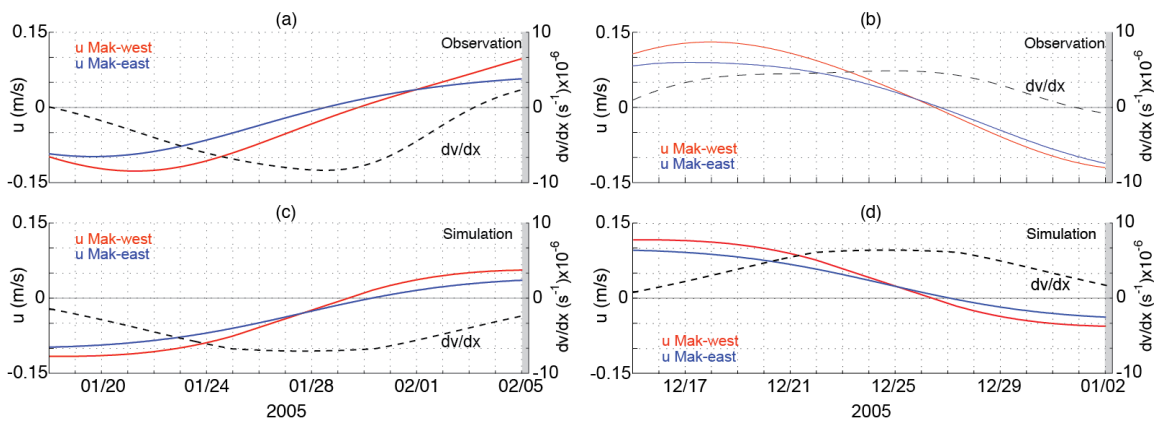
Figure 8. Observation and simulation of across-strait flow (*u*) and relative vorticity

(d*v*/d*x*) varying at 20-40 days at Mak-West and Mak-East mooring sites, which

corresponds with anticyclonic and cyclonic eddy currents. (a, c) displays temporal

variability of real and theoretical anticyclonic eddy respectively, while (b, d)

demonstrates time series of observed and modeled cyclonic eddy respectively.

750

751

752

753

754

755

756

757

758

759

760

761

762
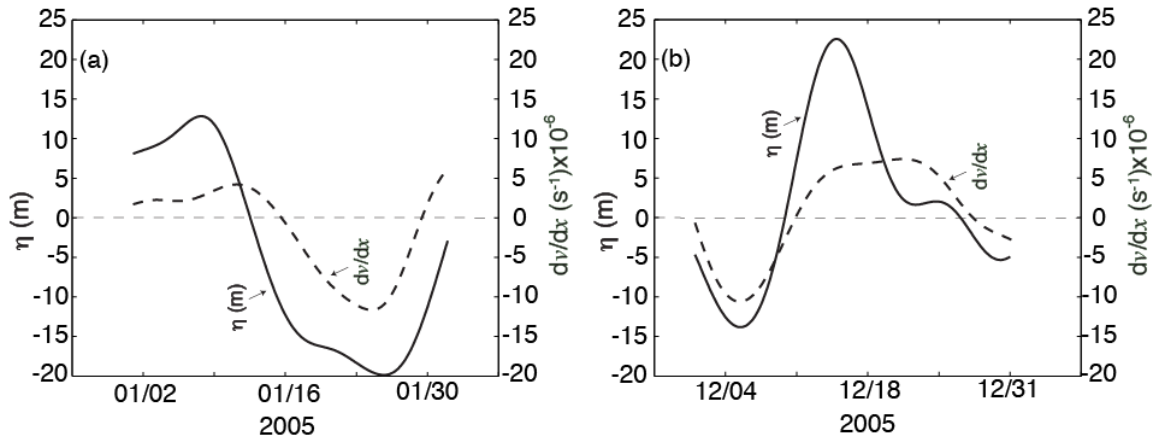
Figure 9. Temporal variability of relative vorticity (dv/dx) and isotherm vertical

displacement (η) at depth of 150 m observed from the moorings in the Labani Channel.

(a) demonstrates how a motion with -dv/dx corresponds with a minimum η on 24 January

2005, while (b) illustrates the relationship between a +dv/dx motion and a maximum η on

17 December 2005.

768

769

770

771

772

773

774

775

776

777

778

779

780
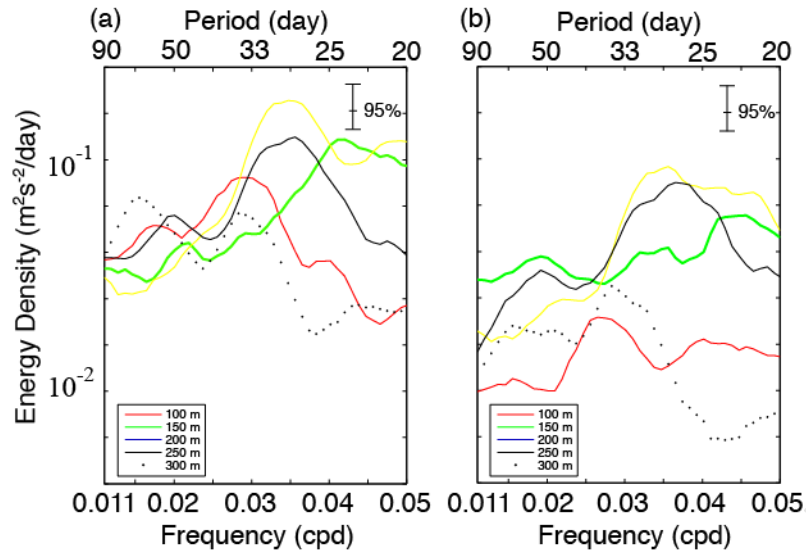
Figure 10. Multitaper spectral estimates of simulated u' at intraseasonal timescales for

several depths at the Mak-West (a) and Mak-East (b) locations in Makassar Strait. Error

bars on the spectral estimates mark the 95% confidence level.

784

785

786

787

788

789

790

791

792

793

794

795
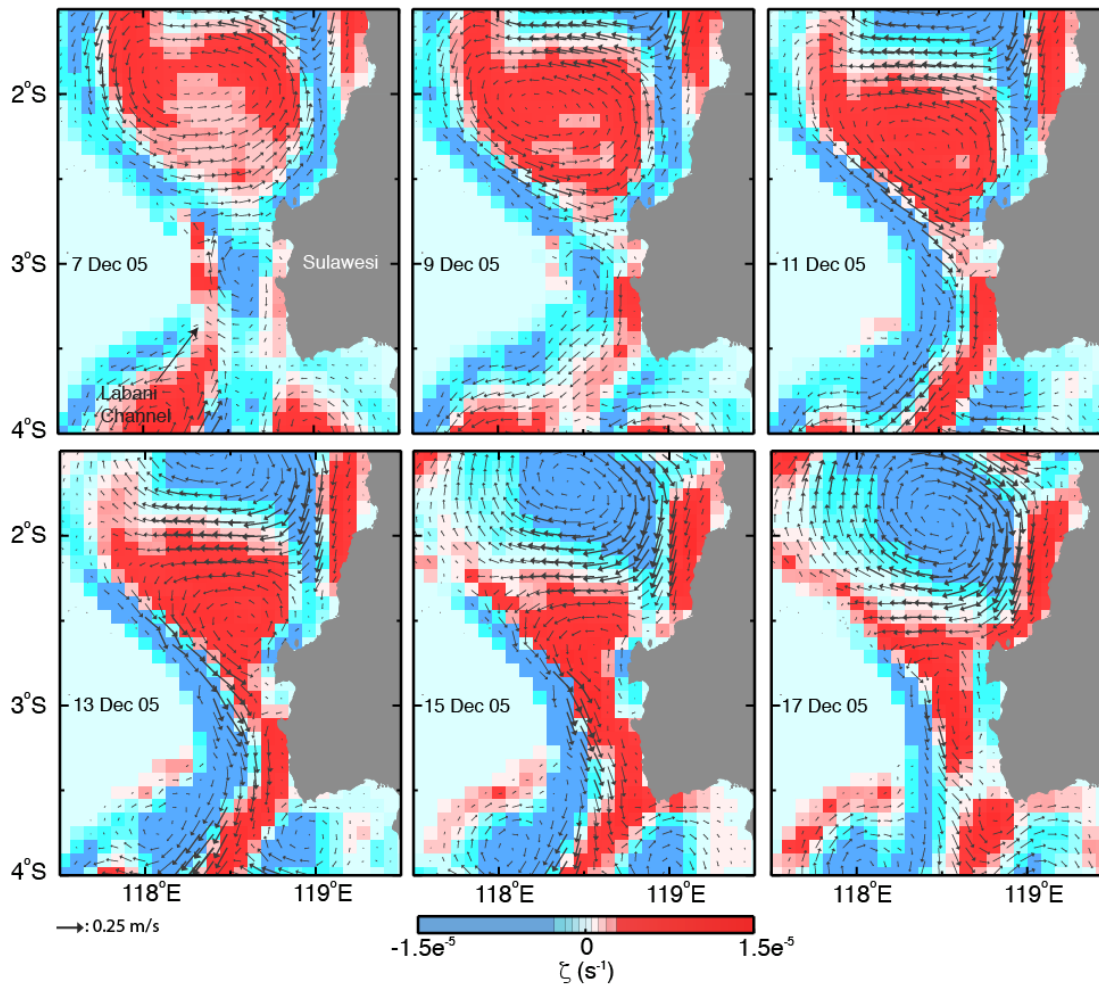
Figure 11. Snapshots of the model horizontal flow field (arrow) and its corresponding vorticity field (in color) at 250 m in the vicinity of the Labani Channel for several days in December 2005. The current vectors are for periods of 20-40 days. The stars denote the mooring sites.
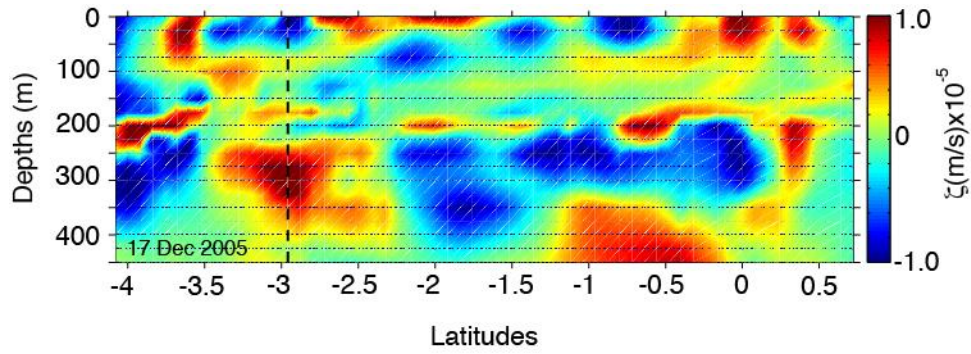
806

807   Figure 12. The model z' plot for several depths along a transect in Makassar Strait

808   shown in Figure 1, simulated on 17 December 2005. The z' time series are computed

809   using horizontal velocities for intraseasonal timescales. The dashed line indicates the

810   latitude of the mooring location in the Labani Channel.
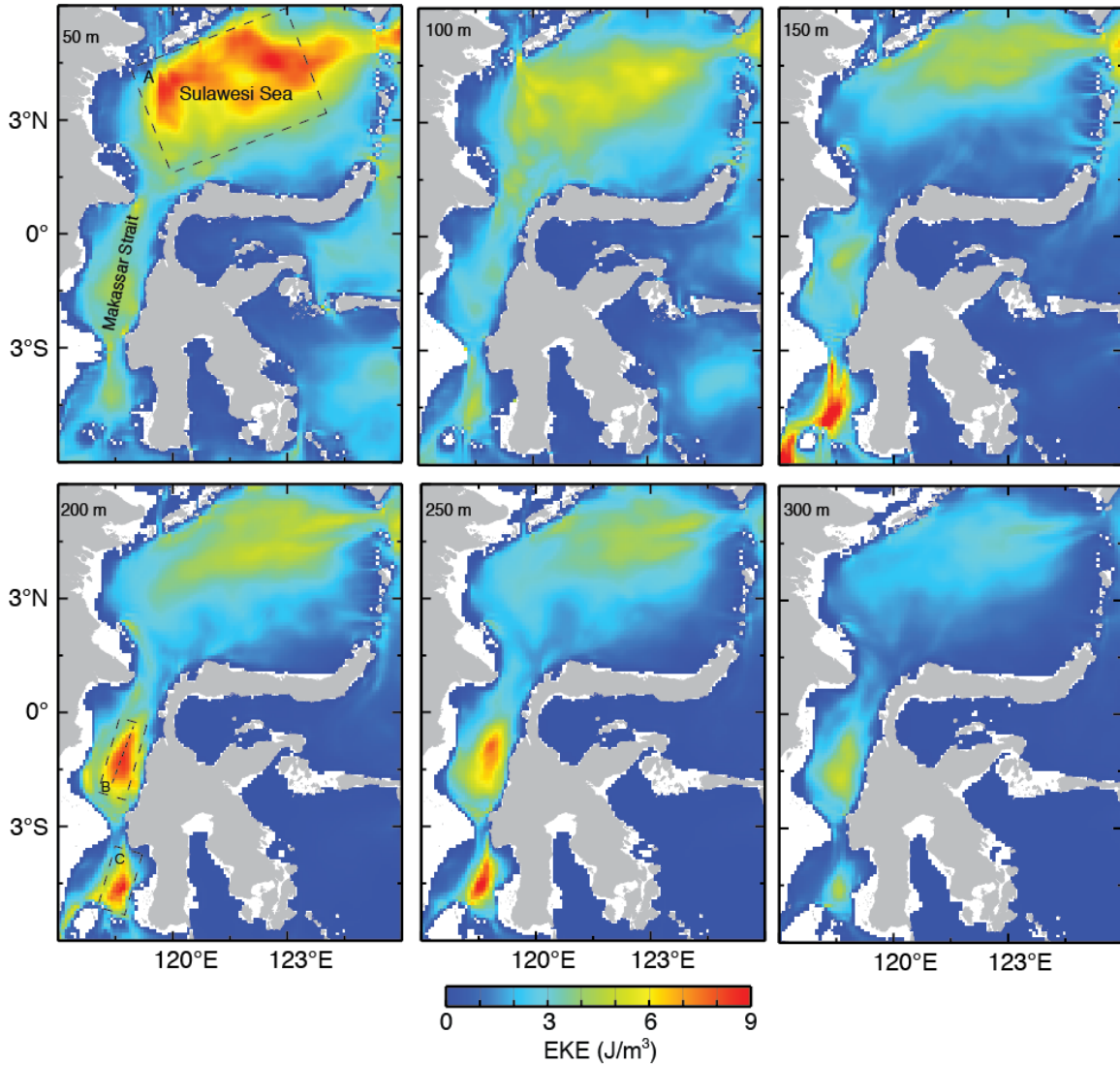
811

812

813

814

815

816

817

818

819

820

821

822

823

824

Figure 13. Plots of the averaged EKE simulated at several depths within the Makassar

Strait and Sulawesi Sea thermocline. The mean EKE is computed for a 3-year period

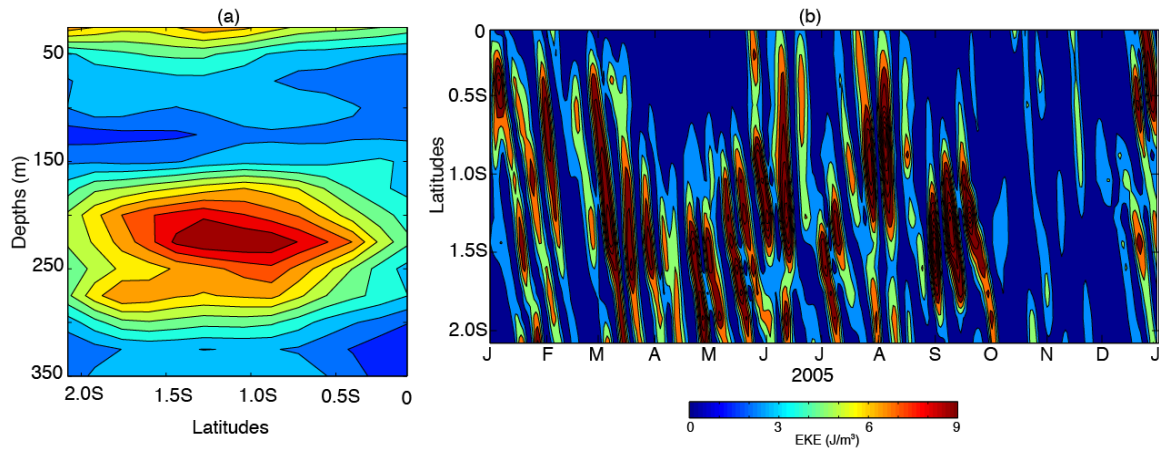from 2004 to 2006. Dashed box represents a region with the most energetic EKE.

834

835 Figure 14. (a) A vertical distribution plot of the mean EKE simulated at several latitudes

836 within zone B given in Figure 13. (b) The temporal variability of the model EKE at depth

837 of 250 m for several latitudes along a transect within zone B shown in Figure 13.

838

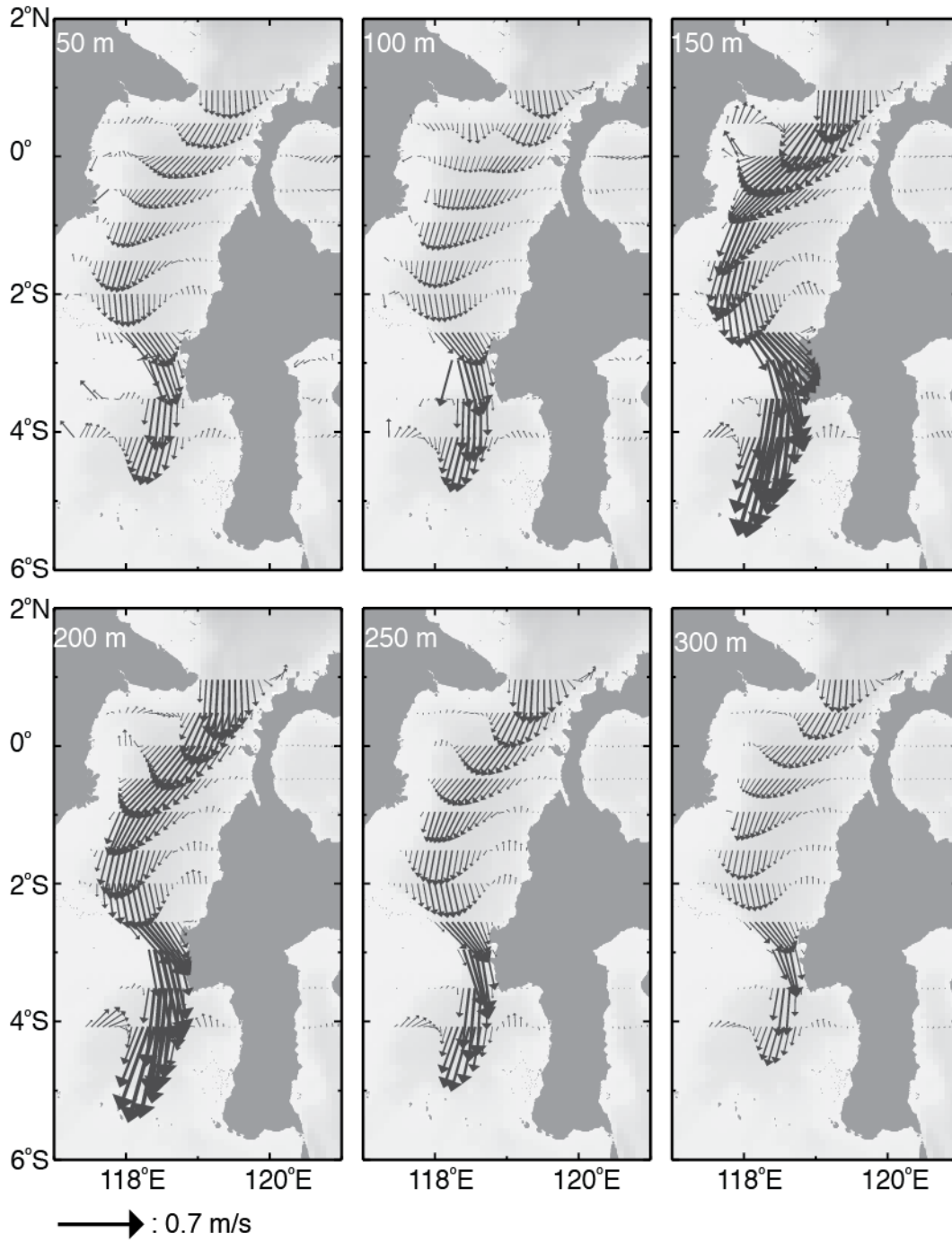839

840

841

842

843

844

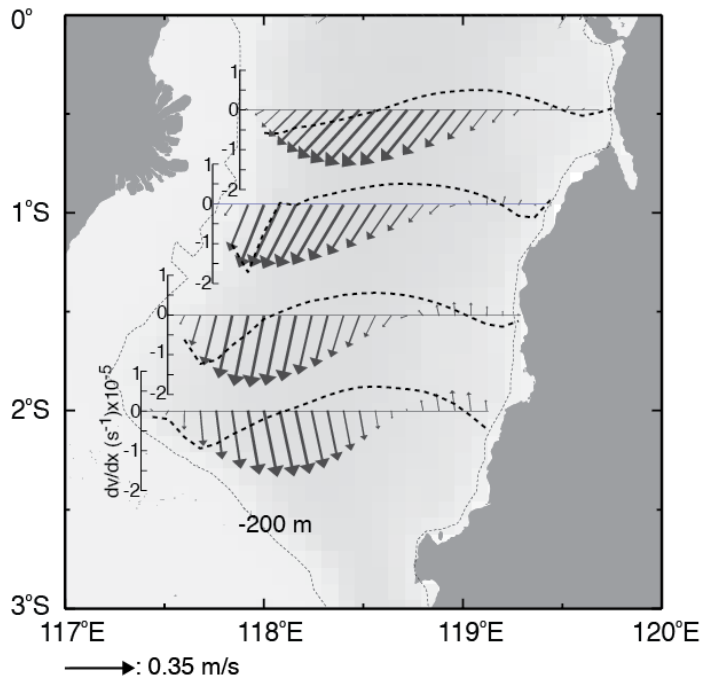845

846

847

848

849

850

851

852

853   Figure 15. The model background flow at several depths simulated in the Makassar Strait

854   thermocline. The mean flow is obtained through applying a butterworth low-pass filter to

855   the model raw data with a cutoff period of 90-day.

856

857

858 Figure 16. The model background flow and relative vorticity at depth of 200 m simulated

859 within latitudes of 0.5°-2°S. The mean flow is obtained through applying a butterworth

860 low-pass filter to the model raw data with a cutoff period of 90-day.

Highlights
>We examine the characteristics and plausible genesis of the 20-40 day variability in Makassar Strait. >The 20-40 day variability is evident in the across-strait flow, relative vorticity and in the vertical displacements of isotherms. > The 20-40 day variability is trapped beneath the depth of the strongest stratification. >We propose that the 20-40 day features are expressions of advected cyclonic and anti-cyclonic eddies. >An eddy-resolving model indicates that the upstream instability of the background flow within Makassar Strait is the energy source for the eddies.